

Local pair natural orbitals for excited states

Benjamin Helmich and Christof Hättig

Citation: J. Chem. Phys. **135**, 214106 (2011); doi: 10.1063/1.3664902
View online: http://dx.doi.org/10.1063/1.3664902
View Table of Contents: http://jcp.aip.org/resource/1/JCPSA6/v135/i21
Published by the American Institute of Physics.

Related Articles

Ab initio calculations of the electronic states of AsH2 including dissociation characteristics
J. Chem. Phys. 135, 244303 (2011)

Analytic derivative couplings between configuration-interaction-singles states with built-in electron-translation factors for translational invariance
J. Chem. Phys. 135, 234105 (2011)

Communication: Extended multi-state complete active space second-order perturbation theory: Energy and nuclear gradients
J. Chem. Phys. 135, 081106 (2011)

Communication: Configuration interaction singles has a large systematic bias against charge-transfer states
J. Chem. Phys. 135, 071104 (2011)

Excited-state geometries and vibrational frequencies studied using the analytical energy gradients of the direct symmetry-adapted cluster–configuration interaction method. I. HAX-type molecules
J. Chem. Phys. 135, 044316 (2011)

Additional information on J. Chem. Phys.

Journal Homepage: http://jcp.aip.org/
Journal Information: http://jcp.aip.org/about/about_the_journal
Top downloads: http://jcp.aip.org/features/most_downloaded
Information for Authors: http://jcp.aip.org/authors

ADVERTISEMENT



Downloaded 09 Jan 2012 to 134.147.252.238. Redistribution subject to AIP license or copyright; see http://jcp.aip.org/about/rights_and_permissions

Local pair natural orbitals for excited states

Benjamin Helmich[a] and Christof Hättig[b]
Lehrstuhl für Theoretische Chemie, Ruhr-Universität Bochum, 44801 Bochum, Germany

(Received 24 September 2011; accepted 9 November 2011; published online 6 December 2011)

We explore how in response calculations for excitation energies with wavefunction based (e.g., coupled cluster) methods the number of double excitation amplitudes can be reduced by means of truncated pair natural orbital (PNO) expansions and localized occupied orbitals. Using the CIS(D) approximation as a test model, we find that the number of double excitation amplitudes can be reduced dramatically with minor impact on the accuracy if the excited state wavefunction is expanded in state-specific PNOs generated from an approximate first-order guess wavefunction. As for ground states, the PNO truncation error can also for excitation energies be controlled by a single threshold related to generalized natural occupation numbers. The best performance is found with occupied orbitals which are localized by the Pipek-Mezey localization. For a large test set of excited states we find with this localization that already a PNO threshold of 10^{-8}–10^{-7}, corresponding to an average of only 40–80 PNOs per pair, is sufficient to keep the PNO truncation error for vertical excitation energies below 0.01 eV. This is a significantly more rapid convergence with the number doubles amplitudes than in domain-based local response approaches. We demonstrate that the number of significant excited state PNOs scales asymptotically linearly with the system size in the worst case of completely delocalized excitations and sub-linearly whenever the chromophore does not increase with the system size. Moreover, we observe that the flexibility of state-specific PNOs to adapt to the character of an excitation allows for an almost unbiased treatment of local, delocalized and charge transfer excited states. © *2011 American Institute of Physics*. [doi:10.1063/1.3664902]

I. INTRODUCTION

The coupled cluster response theory[1–5] approach for the computation of excitation energies[6] and excited state properties is size-consistent and converges systematically towards the full configuration interaction (CI) limit when climbing up the hierarchy of approximate coupled cluster (CC) models CCS (singles),[7,8] CC2,[9] CCSD (singles and doubles),[10] CC3,[11] up to arbitrary order.[12,13] For higher orders, however, the gain in accuracy is accompanied by an unfortunate steep scaling with the system size $\mathcal{N}$, e.g., $\mathcal{O}(\mathcal{N}^6)$ for CCSD, which hinders the application of these methods to extended systems. Various approaches to reduce the computational costs of correlated wavefunction methods by exploiting the locality of dynamic electron correlation have been proposed in the literature. In particular, for ground state energies, important examples are techniques based on integral-screening[14–17] and incremental schemes.[18–20] The most prominent and approved approaches are probably those based on the local correlation approach initially proposed by Pulay in the 1980s,[21] where excitations for a pair of localized occupied orbitals i, j are restricted to projected atomic orbitals (PAOs) that are spatially close to i and j. The domain-based local approach has later been applied extensively to coupled cluster methods by Werner, Schütz and co-workers for the ground state[22–24] as well as excited states.[25–28] Besides domain-based local approaches, excitation energies at the CCSD level for extended systems have recently become available in the context of incremental schemes.[29]

We here present an alternative local approach for an efficient and accurate computation of excitation energies which uses a truncated expansion in pair natural orbitals (PNOs). First reported as pseudo-natural orbitals,[30] PNOs became very popular in the 1970s,[31–41] and lead to a tremendous reduction of the virtual space for calculations using the second-order Møller-Plesset perturbation theory (MP2), coupled electron pair approximation (CEPA), and approximate CI models. Introducing only moderate truncation errors in the correlation energy, the PNO approach facilitated calculations of systems that could not be performed with conventional methods at that time. PNOs have later been fallen into disuse because the integral transformation from the virtual into the PNO space emerged as an acute computational and storage bottleneck. Recently, the use of PNOs has been revived by Neese *et al.* for the CEPA (Ref. 42) and CCSD (Ref. 43) model in combination with the resolution of the identity (RI) approximation for the two-electron integrals[44,45] to bypass these bottlenecks. By their recent work, Neese *et al.* showed that the LPNO-CEPA and LPNO-CCSD method is capable to produce smooth potential energy surfaces which encourages the development of analytic gradient techniques for PNO based correlation methods. Moreover, the PNO approach has lately been applied to compress the space of both virtual and complementary auxiliary orbitals within the framework of explicitly correlated methods.[46]

PNOs present a way to automatically construct very compact virtual spaces through the PNO analysis of a correlated

[a]Electronic mail: benjamin.helmich@rub.de.
[b]Electronic mail: christof.haettig@rub.de.

 © 2011 American Institute of Physics

Downloaded 09 Jan 2012 to 134.147.252.238. Redistribution subject to AIP license or copyright; see http://jcp.aip.org/about/rights_and_permissions

approximate wavefunction. The accuracy can be controlled by a single parameter, which is the occupation number threshold of the PNO truncation. Besides avoiding technical difficulties in choosing spatial domains, the inherent self-adaptivity of PNOs makes them attractive for problems which require an unbiased treatment of local and non-local effects. This is particularly the case when it comes to the calculation of electronic excitation energies with response methods, which is the subject of the present work.

To explore how truncated PNO expansions can be applied for the calculation of excitation energies in the framework of response theory we chose as model the perturbative doubles correction[47] (D) to configuration interaction singles (CIS) excitation energies. CIS(D) is one of the computationally simplest correlated wavefunction approaches for the calculation of electronic excitation energies with a strong relation to coupled cluster response theory. It has a computational complexity comparable to MP2 and has in common with MP2 and coupled cluster methods that it is size-consistent and yields results which are correct through second-order in the electron fluctuation potential.

Similar as MP2 is often used to generate a first-order guess for the ground state doubles amplitudes for higher-order methods as, e.g., CEPA and CCSD, also CIS(D) can be used to generate a first-order guess for the doubles part of the excitation vector in coupled cluster linear response calculations. It is, thus, a perfect model to study how the technique of truncated PNO expansions can be transferred from the ground state to excited states in the framework of response theory and in particular the calculation of excitation energies.

In the present work, we focus on the construction of state-specific truncated PNO expansions for the excitation operator which describes in response theory the transition from the correlated ground to the correlated excited state and the analysis of convergence behavior of truncated PNO expansions for vertical excitation energies where CIS(D) is used as computation model. In Sec. II, we describe how to obtain PNOs from an approximate first-order guess for the excitation operator with emphasis on the similarity between ground and excited states and present working equations for a LPNO-CIS(D) method. Details of the implementation are given in Sec. III. In Sec. IV, we examine the influence of the occupied orbital space on the convergence of the PNO expansion and investigate whether it is necessary to construct state-specific PNOs for excited states. Furthermore, we investigate the scaling of the number of PNOs kept in the expansion with the size of the chromophore and the total system for typical localized and delocalized excitations. We also show that state-specific PNOs are capable to describe excitations to charge transfer states almost as accurately as local valence excitations. In Sec. V, we summarize our results and give an outline of forthcoming work.

II. THEORY

A. MP2-PNOs for the ground state

For closed-shell systems the MP2 energy correction is given by

$$E = \sum_{i \le j} \frac{2}{1+\delta_{ij}} \sum_{ab} L_{ab}^{ij} t_{ab}^{ij}, \tag{1}$$

with the doubles amplitudes

$$t_{ab}^{ij} = -\frac{K_{ab}^{ij}}{\varepsilon_a + \varepsilon_b - \varepsilon_i - \varepsilon_j} \tag{2}$$

and the two-electron integrals $K_{ab}^{ij} = (ia|jb)$ and $L_{ab}^{ij} = 2K_{ab}^{ij} - K_{ba}^{ij}$. In Eq. (2), ε_p denote the Hartree-Fock (HF) orbital energies of canonical molecular orbitals (MOs) p for the occupied $p = i, j$ and virtual space $p = a, b$. PNOs are defined as linear combinations of virtual orbitals,

$$|\bar{a}\rangle = \sum_a |a\rangle d_{a\bar{a}}^{ij}, \tag{3}$$

which are chosen such that they diagonalize the contribution D_{ab}^{ij} of the pair ij to the one-electron density matrix

$$\sum_{ab} d_{a\bar{a}}^{ij} D_{ab}^{ij} d_{b\bar{b}}^{ij} = n_{\bar{a}}^{ij} \delta_{\bar{a}\bar{b}} \tag{4}$$

The eigenvalues of D_{ab}^{ij} are the natural orbital occupation numbers $n_{\bar{a}}^{ij}$, which are positive and, when sorted in descending order, converge rapidly towards zero. At the MP2 level PNOs are calculated from the pair contributions to the density matrix in Eq. (4) constructed from the first-order wave function,[42] which are given by

$$D_{ab}^{ij} = \frac{2}{N_{ij}} \sum_c \left(u_{ac}^{ij} t_{bc}^{ij} + u_{ca}^{ij} t_{cb}^{ij} \right), \tag{5}$$

$$N_{ij} = 1 + \frac{2}{1+\delta_{ij}} \sum_{ab} u_{ab}^{ij} t_{ab}^{ij}, \tag{6}$$

$$u_{ab}^{ij} = 2t_{ab}^{ij} - t_{ba}^{ij}. \tag{7}$$

From the definition of the PNOs in Eq. (4) it is evident that PNOs for a specific pair ij of occupied MOs are orthogonal to each other while the overlap between PNOs of different pairs is given by

$$S_{\bar{a}\bar{b}}^{ij,kl} = \sum_c d_{c\bar{a}}^{ij} d_{c\bar{b}}^{kl}. \tag{8}$$

The transformation from canonical virtual MOs to PNOs by means of Eq. (3) and vice versa can be used to define a projector onto the PNO space of a pair ij

$$\hat{Q}_{ab}^{ij} = \sum_{\bar{c}} d_{a\bar{c}}^{ij} d_{b\bar{c}}^{ij}, \tag{9}$$

which becomes the identity δ_{ab} if no PNOs are discarded.

The closed-shell MP2 energy correction for a truncated PNO expansion can be conveniently defined by projecting the doubles amplitudes of a given pair ij to its own PNO basis:

$$\begin{aligned} E &= \sum_{i \le j} \frac{2}{1+\delta_{ij}} \sum_{ab} \sum_{a'b'} L_{ab}^{ij} \hat{Q}_{aa'}^{ij} t_{a'b'}^{ij} \hat{Q}_{b'b}^{ij} \\ &= \sum_{i \le j} \frac{2}{1+\delta_{ij}} \sum_{\bar{a}\bar{b}} L_{\bar{a}\bar{b}}^{ij} t_{\bar{a}\bar{b}}^{ij}. \end{aligned} \tag{10}$$

Downloaded 09 Jan 2012 to 134.147.252.238. Redistribution subject to AIP license or copyright; see http://jcp.aip.org/about/rights_and_permissions

The PNOs with large occupation numbers are located in the same region of space as the underlying pair *ij* of occupied MOs.[31,32,42] In particular, with localized MOs (LMOs) only a few PNOs per pair *ij* contribute significantly to the wavefunction and energy. This can be exploited to achieve considerable computational savings by truncation of the PNO space. However, the introduction of LMOs in the occupied space causes the occupied-occupied block of the Fock matrix to be nondiagonal and the doubles amplitudes $t^{ij}_{\bar{a}\bar{b}}$ are then determined as solution of the linear equation

$$0 = K^{ij}_{\bar{a}\bar{b}} + \sum_{\bar{c}} \left(F_{\bar{a}\bar{c}} t^{ij}_{\bar{c}\bar{b}} + t^{ij}_{\bar{a}\bar{c}} F_{\bar{c}\bar{b}} \right) - \sum_{k} \sum_{\bar{c}\bar{d}} \left(F_{ik} S^{ij,kj}_{\bar{a}\bar{c}} t^{kj}_{\bar{c}\bar{d}} S^{kj,ij}_{\bar{d}\bar{b}} + S^{ij,ik}_{\bar{a}\bar{c}} t^{ik}_{\bar{c}\bar{d}} S^{ik,ij}_{\bar{d}\bar{b}} F_{kj} \right). \quad (11)$$

B. CIS(D)-PNOs for excited states

Within the CIS(D) method[47] the second-order correction to the zeroth-order CIS excitation energy comprises two parts

$$\omega^{(2)} = \omega_{gs} + \omega_{es}, \quad (12)$$

where electron correlation enters in ω_{gs} via ground state doubles amplitudes and in ω_{es} via excited state doubles amplitudes.

The second-order energy contribution originating from the ground state doubles amplitudes, ω_{gs}, can be conveniently evaluated as

$$\omega_{gs} = \sum_{ai} E^{(0)}_{ai} \rho_{ai}(t^{(1)}_{\mathrm{D}}), \quad (13)$$

with the intermediate

$$\rho_{ai}\left(t^{(1)}_{\mathrm{D}}\right) = -\sum_{j} E^{(0)}_{aj} E_{ji} + \sum_{b} E_{ab} E^{(0)}_{bi} + \sum_{ck} u^{ik}_{ac} \bar{F}_{ck}, \quad (14)$$

where $E^{(0)}_{ai}$ are the zeroth-order excited state singles amplitudes which are normalized as $\sum_{ai}(E^{(0)}_{ai})^2 = 1$. For ease of computation, we used in Eq. (14)

$$\bar{F}_{ck} = \sum_{bj} L^{kj}_{cb} E^{(0)}_{bj}, \quad (15)$$

and the two intermediates

$$E_{ji} = +\sum_{abk} u^{ik}_{ab} K^{kj}_{ba}, \quad (16)$$

$$E_{ab} = -\sum_{cij} u^{ij}_{ac} K^{ji}_{cb}, \quad (17)$$

which depend solely on the two-electron integrals and ground state doubles amplitudes $t^{(1)}_{\mathrm{D}}$, and thus, can be retained independently from a particular excited state as global intermediates.

To truncate the virtual space for the terms that appear in ω_{gs}, pair-specific projectors constructed from the MP2-PNOs of the ground state are employed. The two intermediates that are independent of the excited state are evaluated in the PNO basis as

$$E_{ji} \approx +\sum_{k} \sum_{\bar{a}\bar{b}} u^{ik}_{\bar{a}\bar{b}} \sum_{\bar{c}} S^{ik,kj}_{\bar{b}\bar{c}} \sum_{\bar{d}} K^{kj}_{\bar{c}\bar{d}} S^{kj,ik}_{\bar{d}\bar{a}}, \quad (18)$$

$$E_{ab} \approx -\sum_{ij} \sum_{\bar{a}} d^{ij}_{\bar{a}\bar{a}} \sum_{\bar{c}} u^{ij}_{\bar{a}\bar{c}} \sum_{\bar{b}} K^{ji}_{\bar{c}\bar{b}} d^{ij}_{\bar{b}\bar{b}}. \quad (19)$$

Together with the projection of u^{ik}_{ac} to the (ground state) PNO basis in the third term of $\rho_{ai}(t^{(1)}_{\mathrm{D}})$ this yields

$$\rho_{ai}(t^{(1)}_{\mathrm{D}}) \approx -\sum_{j} E^{(0)}_{aj} E_{ji} + \sum_{b} E_{ab} E^{(0)}_{bi} + \sum_{k} \sum_{\bar{a}} d^{ik}_{\bar{a}\bar{a}} \sum_{\bar{c}} u^{ik}_{\bar{a}\bar{c}} \sum_{c} d^{ik}_{c\bar{c}} \bar{F}_{ck}. \quad (20)$$

For $\bar{F}_{ck}$ the truncated PNO expansion can be exploited by restricting the two-electron integrals in L^{kj}_{cb} to the PNO basis of the pair *kj*:

$$\bar{F}_{ck} \approx \sum_{j} \sum_{\bar{c}} d^{kj}_{c\bar{c}} \sum_{\bar{b}} L^{kj}_{\bar{c}\bar{b}} \sum_{b} d^{kj}_{b\bar{b}} E^{(0)}_{bj}. \quad (21)$$

The expression for ω_{es} is closely related to the equations for the MP2 ground state energy:

$$\omega_{es} = \sum_{i \le j} \frac{1}{1+\delta_{ij}} \sum_{ab} \tilde{L}^{ij}_{ab} E^{ij}_{ab}. \quad (22)$$

In the last equation, $\tilde{L}^{ij}_{ab}$ are modified two-electron integrals

$$\tilde{L}^{ij}_{ab} = 2\tilde{K}^{ij}_{ab} - \tilde{K}^{ij}_{ba}, \quad (23)$$

and E^{ij}_{ab} are the first-order excited state doubles amplitudes

$$E^{ij}_{ab} = -\frac{\tilde{K}^{ij}_{ab}}{\varepsilon_a + \varepsilon_b - \varepsilon_i - \varepsilon_j - \omega^{(0)}}. \quad (24)$$

Compared to the ground state doubles amplitudes in (2), the CIS excitation energy $\omega^{(0)}$ appears supplementary in the orbital denominator of Eq. (24). Furthermore, $\tilde{K}^{ij}_{ab}$ are two-electron integrals which are one-index transformed with the CIS singles amplitudes:[48]

$$\tilde{K}^{ij}_{ab} = -\sum_{k} \left(E^{(0)}_{ak}(ki|bj) + (ai|kj) E^{(0)}_{bk} \right) + \sum_{c} \left(E^{(0)}_{ci}(ac|bj) + (ai|bc) E^{(0)}_{cj} \right). \quad (25)$$

As mentioned before, electron correlation enters into the contribution ω_{es} through the excited state doubles amplitudes E^{ij}_{ab}. We thus propose to construct PNOs separately for each excited state that provide a compact description of the first-order excited state wavefunction $|\Psi^{(1)}_{es}\rangle = \sum_{ijba} E^{ij}_{ab} |\Psi^{ij}_{ab}\rangle$. Similar as for the ground state, also for excited states $|\Psi^{(1)}_{es}\rangle$ accounts already for a large fraction of correlation effects so that a (truncated) basis of PNOs for $|\Psi^{(1)}_{es}\rangle$ can be expected to provide also a compact and accurate basis for higher-order correlation contributions to the wavefunction. This explains the accuracy that is obtained when using approximate PNOs built from first-order wave functions as it has been demonstrated by Neese *et al.* for LPNO-CEPA and LPNO-CCSD.

Downloaded 09 Jan 2012 to 134.147.252.238. Redistribution subject to AIP license or copyright; see http://jcp.aip.org/about/rights_and_permissions

From Eq. (25) it follows that the excited state doubles amplitudes depend (through $E^{(0)}_{ai}$) strongly on the nature of the excited state and can in particular exhibit a long-range character whenever the excitation (i.e., $E^{(0)}_{ai}$) is non-local. Therefore, it is very unlikely that ground state PNOs are an appropriate choice for expanding excited state wavefunctions. We will come back to this point in Sec. IV C.

PNOs for excited states can be obtained by replacing t^{ij}_{ab} by E^{ij}_{ab} in Eqs. (5)–(7)

$$\tilde{D}^{ij}_{ab} = \frac{2}{\tilde{N}_{ij}} \sum_c \left(\tilde{u}^{ij}_{ac} E^{ij}_{bc} + \tilde{u}^{ij}_{ca} E^{ij}_{cb} \right), \tag{26}$$

$$\tilde{N}_{ij} = 1 + \frac{2}{1+\delta_{ij}} \sum_{ab} \tilde{u}^{ij}_{ab} E^{ij}_{ab}, \tag{27}$$

$$\tilde{u}^{ij}_{ab} = 2E^{ij}_{ab} - E^{ij}_{ba}. \tag{28}$$

As ground state PNOs, the excited state PNOs are expanded in canonical virtual MOs and diagonalize the contributions to the density matrices built from the first-order CIS(D) wave function in Eq. (26) for a pair *ij*. Working equations for the energy contribution from the excited state doubles amplitudes, ω_{es}, with PNOs are obtained by projecting E^{ij}_{ab} to the state-specific PNO basis. This leads to the expression

$$\omega_{es} = \sum_{i \le j} \frac{1}{1+\delta_{ij}} \sum_{\bar{a}\bar{b}} \tilde{L}^{ij}_{\bar{a}\bar{b}} E^{ij}_{\bar{a}\bar{b}}, \tag{29}$$

where the amplitudes $E^{ij}_{\bar{a}\bar{b}}$ are the solution of the linear equation

$$\begin{aligned} 0 = {} & \tilde{K}^{ij}_{\bar{a}\bar{b}} - \omega^{(0)} E^{ij}_{\bar{a}\bar{b}} + \sum_{\bar{c}} \left(F_{\bar{a}\bar{c}} E^{ij}_{\bar{c}\bar{b}} + E^{ij}_{\bar{a}\bar{c}} F_{\bar{c}\bar{b}} \right) \\ & - \sum_k \left(F_{ik} S^{ij,kj}_{\bar{a}\bar{c}} E^{kj}_{\bar{c}\bar{d}} S^{kj,ij}_{\bar{d}\bar{b}} + S^{ij,ik}_{\bar{a}\bar{c}} E^{ik}_{\bar{c}\bar{d}} S^{ik,ij}_{\bar{d}\bar{b}} F_{kj} \right). \end{aligned} \tag{30}$$

C. Occupied orbital space for excited states

The applicability of domain-based local methods to excited state response calculations has been hampered by the prevalent non-local character of the electronic excitation that causes an increase of domain sizes or of the domain errors. This issue has been recently addressed by Mata and Stoll[29] for an incremental scheme to compute vertical excitation energies, where a mixed occupied orbital space, built from LMOs and natural transition orbitals[49,50] (NTOs), has been proposed. NTOs facilitate a compact orbital representation for the zeroth-order electronic transition density matrix,

$$E^{(0)}_{ai} = \left\langle \tilde{\Psi}^{(0)}_{ex} \middle| \hat{E}_{ai} \middle| \Psi^{(0)}_{gs} \right\rangle, \tag{31}$$

of the ground state HF wave function $|\Psi^{(0)}_{gs}\rangle$ and excited state CIS contravariant configuration state function $\langle\tilde{\Psi}^{(0)}_{ex}|$ and are obtained through a singular value decomposition (SVD) of the single excitation amplitudes $E^{(0)}_{ai}$ with the eigendecompositions

$$\mathbf{E}^\dagger \mathbf{E} u_i = \lambda_i u_i, \quad i = 1, 2, \ldots, N_o \tag{32}$$

$$\mathbf{E}\mathbf{E}^\dagger v_i = \lambda_i v_i, \quad i = 1, 2, \ldots, N_v, \tag{33}$$

that procure unitary transformation matrices for occupied,

$$\mathbf{U} = (\mathbf{u}_1, \mathbf{u}_2, \ldots, \mathbf{u}_{N_o}) \tag{34}$$

and virtual

$$\mathbf{V} = (\mathbf{v}_1, \mathbf{v}_2, \ldots, \mathbf{v}_{N_v}) \tag{35}$$

canonical molecular orbitals. This new set of orbitals for the occupied and virtual space describes contributions from particle-hole pairs to excited states. If $E^{(0)}_{ai}$ is normalized to $tr(\mathbf{E}\mathbf{E}^\dagger) = 1$ the singular-values of $E^{(0)}_{ai}$

$$[\mathbf{V}^\dagger \mathbf{E} \mathbf{U}]_{ij} = \sqrt{\lambda_i}\delta_{ij} \tag{36}$$

are bound by $0 \le \sqrt{\lambda_i} \le 1$ and give a weight to each particle-hole pair. Usually, $E^{(0)}_{ai}$ can be well approximated by a few dominant contributions to its SVD. A mixed orbital space for occupied orbitals can be constructed by localization of all but the most dominant NTO(s). As already discussed in the work of Mata and Stoll, this mixed localization procedure carries the risk of producing poorly localized molecular orbitals, but this could not be observed in the context of their incremental approach.[29] We investigate the effect of pure and such mixed localization schemes on the convergence of truncated PNO expansions for excited states in Sec. IV A.

III. COMPUTATIONAL DETAILS

The LPNO-CIS(D) approach proposed in Sec. II has been implemented in a development version of the TURBOMOLE program package. The number of PNOs for every pair is determined by truncating the PNO expansion at natural occupation numbers $n^{ij}_{\bar{a}}$ smaller than a user-defined PNO threshold T_{PNO}. Additionally, pairs *ij* are neglected if the corresponding pair contribution to E_{MP2} and ω_{es}, respectively, is smaller than a pair threshold T_{ij}. However, at this point it should be noted that the introduction of a pair threshold is primarily motivated by avoiding the diagonalization of an unnecessarily large number of pair-density matrices in Eqs. (5) and (26) for pairs which would not contribute a single PNO to the truncated PNO space and, therefore, would be discarded anyway. Thus, it has been emphasized in previous works[42,46] that the error introduced by truncating the PNO space can be determined by a single threshold, which is T_{PNO}. For convenience, we have in the present study set both thresholds to the same value in all calculations. Furthermore, the number of NTOs is controlled by the number of eigenvalues λ_i in Eq. (32) which are larger than a user-defined threshold T_{NTO}. In all calculations, where we employed a mixed occupied orbital space as described in Sec. II, NTOs with $\lambda_i < 0.1$ have been omitted.

The HF calculations have been performed with the dscf module,[51] density functional theory (DFT) calculations with the ridft module,[52] and CIS(D) and CC2 calculations with the ricc2 module[53] of the TURBOMOLE program package[54] using the TZVP,[55] def2-TZVP and def2-TZVPP,[56,57] cc-pVDZ and cc-pVTZ,[58] and aug-cc-pVTZ[59] orbital basis sets. For all correlated calculations we made use of the RI approximation for two-electron integrals and their one-index

Downloaded 09 Jan 2012 to 134.147.252.238. Redistribution subject to AIP license or copyright; see http://jcp.aip.org/about/rights_and_permissions

transformed variants[53] using auxiliary basis sets optimized for the corresponding orbital basis sets from Refs. 56, 57, and 60. Furthermore, all core electrons have been kept frozen, i.e., $1s^2$ for C,N, and O atoms, and $1s^2 2s^2 2p^6$ for S and Cl atoms.

The molecular structures for the benchmark set of Schreiber *et al.* were taken from the supporting information of Ref. 61 and the structure of 2,4-dichloro-6-[p-(N,N-diethylamino)biphenylyl]-1,3,5-triazine (DBQ) from the supporting information of Ref. 62. For the tests sets used in Refs. 26 and 27 to benchmark local EOM-CCSD and CC2 implementations the structures were kindly provided by the authors. The structures of all-*trans* conjugated alkenes $C_{2n}H_{2n+2}$ with n = 1, ..., 7 and all-*trans* saturated fatty acids $C_{2n-1}H_{4n-1}COOH$ with n = 1, ..., 7 were optimized at the B3LYP level with the TZVP basis set and are provided in the supporting information.[63]

IV. RESULTS AND DISCUSSION

A. Choice of the occupied space

As pointed out in Sec. II, PNOs which contribute significantly to the correlation energy are located in the vicinity of the underlying localized occupied MOs and, thus, depend on the localization method. For excited states we furthermore know that the most important occupied orbitals should be the occupied space NTOs with the largest singular values. In order to identify the type of occupied orbitals that lead to the most compact PNO expansion we investigated in this study different procedures which employ either the Pipek-Mezey[64] (PM) or the Foster-Boys[65,66] (FB) localization:

1. FB or PM for ground and excited states,
2. PM for the ground state and NTOs for excited states, and
3. FB or PM for the ground state while for excited states the most dominant NTOs are kept and the remaining occupied orbitals are localized (for details see Sec. III).

To evaluate their performance we used a benchmark set proposed in Refs. 61 and 67, which contains 28 organic molecules that are supposed to represent the most important chromophores in organic photochemistry. For these molecules, several vertical excitation energies have been computed, amongst others, with the CC2 model[9] using the TZVP[61] and aug-cc-pVTZ[67] basis sets. In the present study, we have selected for each basis set a subset of singlet states where the CIS(D) and CC2 vertical excitation energies differ by less than 1 eV and are dominated by the same orbital transitions in the CIS and CC2 excited state singles amplitudes, to keep the calculations comparable. A detailed listing of the selected states is given in the supporting information.[63]

For these excited states the mean absolute PNO truncation error in the correlation contribution originating from the excited state doubles amplitudes, ω_{es}, is plotted as a function of the mean number of excited state PNOs using the TZVP (Fig. 1) and the aug-cc-pVTZ basis set (Fig. 2). The mean absolute error and the mean number of PNOs are averaged over all states. The mean number of PNOs has been calculated by averaging over all pairs which give sizeable contributions to ω_{es}. The five data points in each graph correspond to PNO thresholds of 1×10^{-n} with $n = 6, \ldots, 10$ as the number of PNOs increases. For both basis sets the pure localization schemes (1) yield much smaller errors for a given number of PNOs than found with only NTOs (2) and the composite localization schemes (3) where only the most dominant NTOs are kept and all other occupied orbitals are localized. For the latter two approaches we observe that the PNO space is more compact when all NTOs are kept, rather than including only the dominant NTO(s) and localizing the remaining orbitals. Thus, it has to be concluded that using an incomplete set of NTOs corrupts the localization and leads to rather extended PNO spaces. On the other hand, keeping all NTOs would prevent the application of integral pre-screening to reduce

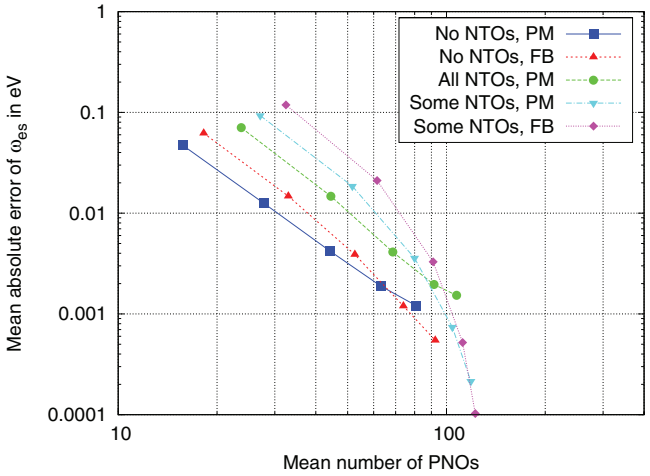


FIG. 1. Mean absolute PNO errors of the ω_{es} contribution to vertical CIS(D)/TZVP excitation energies in eV as a function of the mean number of PNOs per pair for five different occupied orbital spaces. The errors as well as the number of PNOs are averaged over 116 excited states of 28 organic molecules (c.f. Ref. 63). The five data points in each graph correspond to PNO thresholds T_{PNO} of 1×10^{-n} with $n = 6, \ldots, 10$ as the number of PNOs increases. The NTO threshold T_{NTO} is set to 0.1.

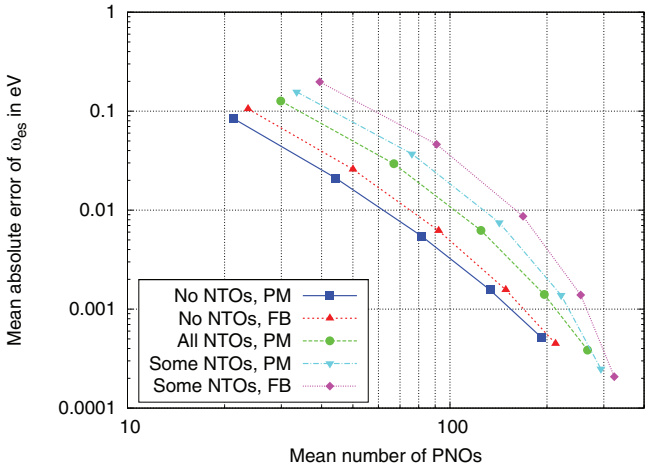


FIG. 2. Mean absolute PNO errors of the ω_{es} contribution to vertical CIS(D)/aug-cc-pVTZ excitation energies in eV as a function of the mean number of PNOs per pair for five different occupied orbital spaces. The errors as well as the number of PNOs are averaged over 91 excited states of 28 organic molecules (c.f. Ref. 63). The five data points in each graph correspond to PNO thresholds T_{PNO} of 1×10^{-n} with $n = 6, \ldots, 10$ as the number of PNOs increases. The NTO threshold T_{NTO} is set to 0.1.

Downloaded 09 Jan 2012 to 134.147.252.238. Redistribution subject to AIP license or copyright; see http://jcp.aip.org/about/rights_and_permissions

further the computational costs. In contrast to the incremental approach for excited states proposed in Ref. 29, it seems that correlation methods with a truncated PNO expansion for excited states do not benefit from such a composite localization approach for occupied MOs. In the following, we will thus restrict the discussion to the scheme where all occupied orbitals are localized. For this scheme we note that from Figs. 1 and 2 it is evident that at least for the organic chromophores covered by the test set the PM localization yields smaller truncation errors for an equal number of PNOs, or rather less PNOs for the same truncation error, than the FB localization. Thus, PM localization seems to be the localization method of choice for excited state PNO calculations. This observation has been confirmed by additional calculations, though results with other occupied spaces are in the following omitted for clarity.

B. Contributions to the excitation energy

In previous PNO studies on the electronic ground state, it has been shown by Neese *et al.* for LPNO-CEPA[42] and LPNO-CCSD,[43] and by Tew *et al.* for LPNO-MP2-F12[46] that the PNO error decreases smoothly and monotonically towards zero as the number of PNOs increases. However, this is not expected for LPNO-CIS(D) because the two contributions ω_{gs} and ω_{es} have – due to their different physical origin – opposite signs: ω_{gs} accounts for ground state correlation which stabilizes the ground state and thereby increases the excitation energy. Thus, ω_{gs} is positive. In contrast to this, ω_{es} has a negative sign which has its origin in the inclusion of excited state correlation which decreases the excitation energy since it stabilizes the excited state. An incomplete PNO space results in negative PNO truncation errors for ω_{gs} and positive PNO truncation errors for ω_{es}. The total PNO error can thus have a negative or positive sign, depending on the balance between the two contributions, and does not necessarily decrease monotonically.

We have plotted for the previous test set the absolute errors of the ground state ω_{gs} and excited state contributions ω_{es} as well as the absolute error in $\omega^{(2)} = \omega_{gs} + \omega_{es}$ for the TZVP and the aug-cc-pVTZ basis set in Figs. 3 and 4. As can be seen from these figures, the absolute errors in the ground state ω_{gs} and excited state ω_{es} contributions to $\omega^{(2)}$ decrease both smoothly and monotonically towards zero with an increasing number of PNOs. The opposite signs of their truncation errors, however, cause the absolute errors of $\omega^{(2)}$ to decrease non-monotonically. The two errors usually have the same order of magnitude but opposite signs which leads to an advantageous error compensation for $\omega^{(2)}$. Due to this compensation, we observe for both basis sets and every state in the test set an absolute error in $\omega^{(2)}$ which is less than ≈ 0.01 eV with a PNO threshold of 1×10^{-8} and PM localization (see supporting information[63]). This accuracy is surely sufficient if one considers that even for methods which account for connected triple excitations, as, e.g., CC3, the intrinsic error[6] for states dominated by single excitations is still in the same order of magnitude. This high accuracy is also reflected by the statistical measures for the PNO error in $\omega^{(2)}$ tabulated in Table I. For our recommended PNO threshold of 1×10^{-8} the mean absolute PNO error is less than the maximum PNO error by a factor of about 5.

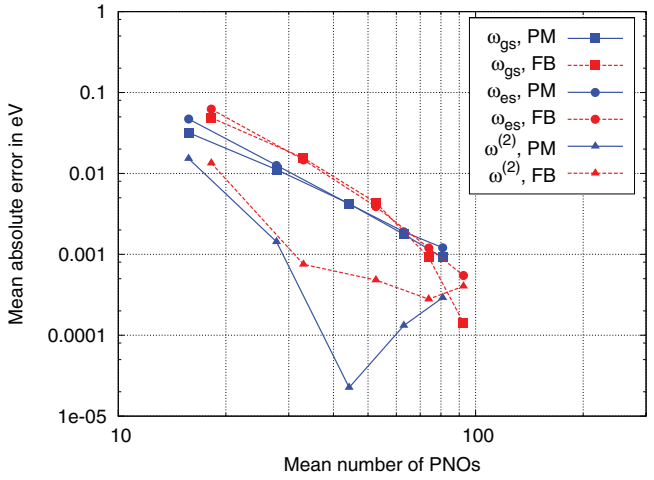


FIG. 3. Absolute PNO errors of vertical CIS(D)/TZVP excitation energies $\omega^{(2)}$ and its ground ω_{gs} and excited state contributions ω_{es} in eV as a function of the mean number of PNOs per pair for the PM and FB localization. The errors as well as the number of PNOs are averaged over 116 excited states of 28 organic molecules (c.f. Ref. 63). The five data points in each graph correspond to a PNO thresholds of 1×10^{-6} to 1×10^{-10} by increments of $\frac{1}{10}$ as the mean number of PNOs increases.

C. PNOs for excited states

The state-specific PNOs as proposed in Sec. II introduce further computational costs, which could in principle be avoided by projecting both ground state (t_{ab}^{ij}) and excited state (E_{ab}^{ij}) doubles amplitudes to the ground state PNO space. To explore whether this approximation affects the PNO truncation error we compared the absolute errors for ω_{es} caused by

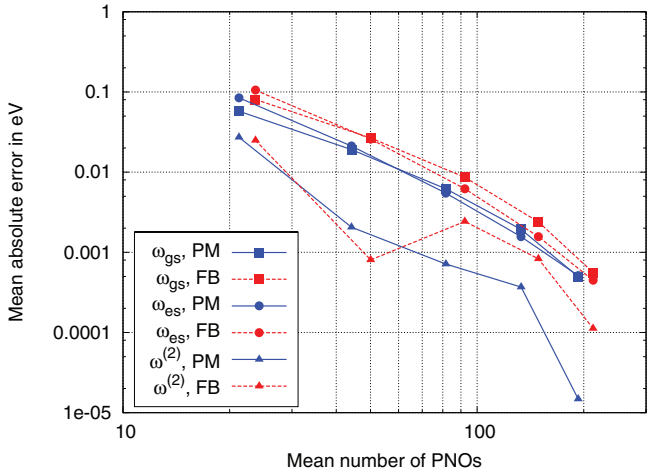


FIG. 4. Absolute PNO errors of vertical CIS(D)/aug-cc-pVTZ excitation energies $\omega^{(2)}$ and its ground ω_{gs} and excited state contributions ω_{es} in eV as a function of the mean number of PNOs per pair for the PM and FB localization. The errors as well as the number of PNOs are averaged over 91 excited states of 28 organic molecules (c.f. Ref. 63). The five data points in each graph correspond to a PNO thresholds of 1×10^{-6} to 1×10^{-10} by increments of $\frac{1}{10}$ as the mean number of PNOs increases.

Downloaded 09 Jan 2012 to 134.147.252.238. Redistribution subject to AIP license or copyright; see http://jcp.aip.org/about/rights_and_permissions

TABLE I. Statistics on mean numbers of PNOs per pair N_{PNO}/N_{ij} and PNO errors of $\omega^{(2)}$ in eV for a benchmark set containing 116 excited states calculated with the TZVP and 91 excited states calculated with the aug-cc-pVTZ basis set (see Ref. 63). For N_{PNO}/N_{ij} the mean number AV, standard deviation STD, and maximum number MAX of the benchmark set are tabulated. For the PNO errors the mean number AV, standard deviation STD, mean absolute error MAE, and maximum error MXE of the benchmark set are tabulated. The PNO threshold T_{PNO} was set to 10^{-n} with $n = 6, \ldots, 10$. Occupied orbitals were localized with the PM localization.

	N_{PNO}/N_{ij}			$\omega^{(2)}_{PNO} - \omega^{(2)}_{CMO}$			
$-\log(T_{PNO})$	AV	STD	MAX	AV	STD	MAE	MXE
			TZVP				
6	15.0	3.7	25.1	0.01563	0.01776	0.01847	0.07716
7	26.8	7.5	44.5	0.00182	0.00646	0.00521	0.02194
8	43.8	11.8	75.5	−0.00002	0.00268	0.00188	0.00854
9	63.4	15.7	112.0	−0.00004	0.00114	0.00074	0.00441
10	82.2	19.2	142.4	0.00010	0.00067	0.00042	0.00372
			aug-cc-pVTZ				
6	21.3	5.7	34.1	0.02719	0.02480	0.03018	0.09685
7	44.2	13.0	66.4	0.00206	0.00810	0.00666	0.02441
8	81.6	22.7	122.4	−0.00071	0.00329	0.00236	0.01027
9	133.1	32.6	190.7	−0.00037	0.00117	0.00083	0.00375
10	192.9	40.0	283.5	0.00001	0.00037	0.00023	0.00193

truncated excited state CIS(D)- and ground state MP2-PNO expansions for three different excited states (acetone S_7 ($\sigma \rightarrow \pi^*$), adenine S_8 ($n \rightarrow \pi^*$), and benzoquinone S_4 ($\pi \rightarrow \pi^*$)) that have different characters (all three states are part of the benchmark set of the Mühlheim group[61,67]). As shown in Fig. 5 the PNO truncation errors in ω_{es} are 1 to 2 orders of magnitude larger when using ground state rather than excited state PNOs. A reasonable accuracy of ≈0.01 eV can with ground state PNOs only be retained if one accepts a dramatic increase in the number of PNOs. The additional costs caused by constructing a PNO basis for each excited state and transforming some integrals and intermediates into this state-specific PNO basis will for calculations of excitation energies with higher-order methods like CCSD by far be overcompensated by savings due to the reduction of the PNO space. Thus, it turns out that for efficient calculations of excitation energies the exclusive use of ground state PNOs is impractical and state specific PNOs as introduced in Sec. II are the preferred choice.

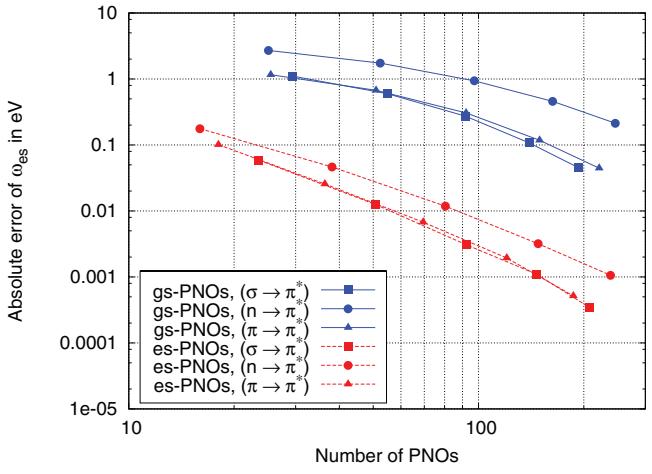


FIG. 5. Absolute PNO errors of the ω_{es} contribution to vertical CIS(D)/aug-cc-pVTZ excitation energies in eV as a function of the mean number of PNOs per pair using ground or excited state PNOs respectively. The occupied orbitals are localized by PM. Excited states are: acetone S_7 ($\sigma \rightarrow \pi^*$), adenine S_8 ($n \rightarrow \pi^*$), and benzoquinone S_4 ($\pi \rightarrow \pi^*$). The five data points in each graph correspond to PNO thresholds T_{PNO} of 1×10^{-n} with $n = 6, \ldots, 10$ as the number of PNOs increases.

D. Scaling of the PNO expansion with the system size

Probably the most appealing effect of PNOs is their black-box character in which they adapt to the short-range behavior of electron correlation (at least for insulators) as the number of PNOs which contribute significantly scales eventually linearly with the system size. This is primarily reached by a rapid convergence of the natural occupation numbers towards zero, especially for distant pairs. To investigate the dependence of PNO expansions on the system size, we first considered the all-*trans* conjugated alkenes $C_{2n}H_{2n+2}$ with $n = 1, \ldots, 7$. Since the chromophore region is extended over (nearly) the whole molecule, conjugated alkenes are a tough test case, especially for local approaches to excited states. In Fig. 6, we plotted the PNO truncation errors for the ground state S_0 and the first excited state S_1 against the total number of PNOs divided by the number of carbon atoms which ideally becomes independent of the system size. For the ground state as well as the first excited state the number of PNOs per carbon atom tends to converge to a constant value. This convergence is fast for the loosest PNO threshold $T_{\mathrm{PNO}} = 1 \times 10^{-6}$ and somewhat slower for tighter PNO thresholds.

We also investigated the scaling for a second class of molecules with the system size, namely the all-*trans* saturated fatty acids $C_{2n-1}H_{4n-1}COOH$ with n = 1, …, 7. Here, the chromophore is located at the carboxyl group and remains spatially confined and only the non-chromophore part

Downloaded 09 Jan 2012 to 134.147.252.238. Redistribution subject to AIP license or copyright; see http://jcp.aip.org/about/rights_and_permissions

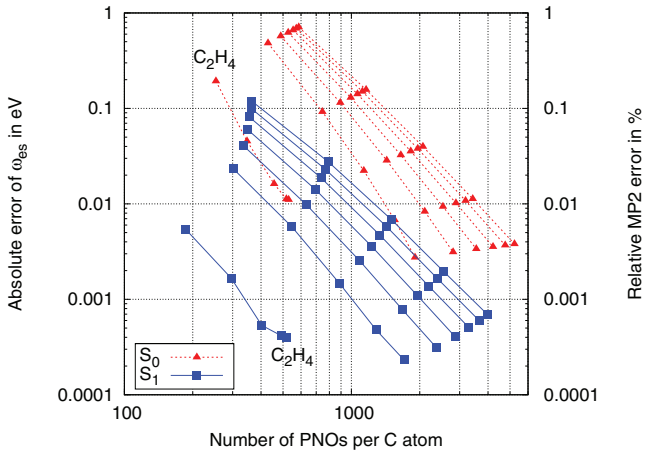


FIG. 6. Absolute PNO errors of the ω_{es} contribution to vertical CIS(D)/TZVP excitation energies in eV of the first excited state S_1 and relative PNO errors of the MP2/TZVP correlation energy in % of the ground state S_0 of the all-*trans* conjugated alkenes $C_{2n}H_{2n+2}$ with $n = 1, \ldots, 7$ as a function of the total number of PNOs per carbon atom. The occupied orbitals are localized by PM. The five data points in each graph correspond to PNO thresholds T_{PNO} of 1×10^{-n} with $n = 6, \ldots, 10$ as the number of PNOs increases.

increases with n. For this class of molecules one expects therefore that, on the one hand, the number of significant ground state PNOs scales linearly with the system size but, on the other hand, the number of significant excited state PNOs should reach a constant limit. This is exactly what is observed in Fig. 7, where the PNO truncation error is plotted against the total number of PNOs for the ground state S_0 and the first excited state S_1. In case of the ground state, the number of significant PNOs divided by the number of carbon atoms is approximately constant. For S_1 the total number of significant PNOs converges quickly to a constant which can be easily attributed to the constant size of the chromophore region restricted to the carboxyl group. Since in practice most of the extended systems that spectroscopists are interested in exhibit

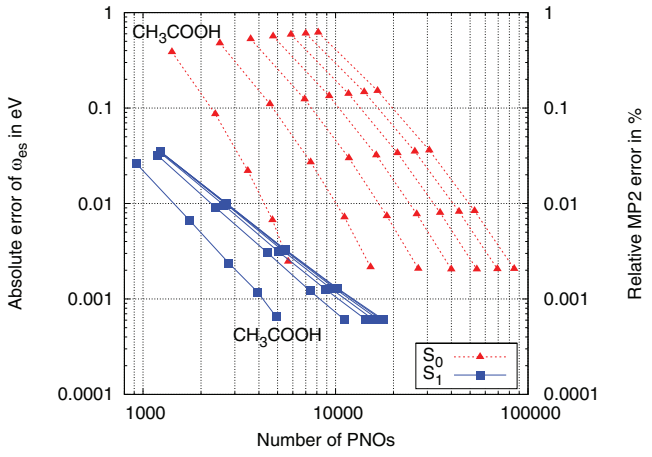


FIG. 7. Absolute PNO errors of the ω_{es} contribution to vertical CIS(D)/TZVP excitation energies in eV of the first excited state S_1 and relative PNO errors of the MP2/TZVP correlation energy in % of the ground state S_0 of the all-*trans* saturated fatty acids $C_{2n-1}H_{4n-1}COOH$ with $n = 1, \ldots, 7$ as a function of the total number of PNOs. The occupied orbitals are localized by PM. The five data points in each graph correspond to PNO thresholds T_{PNO} of 1×10^{-n} with $n = 6, \ldots, 10$ as the number of PNOs increases.

a considerable amount of non-chromophore groups, the use of excited state PNOs will eventually pay off. However, it should be fairly remarked that for second-order methods excitation energies comprise of two parts depending on either ground or excited state PNOs and ground state PNOs are still located in all parts of the molecule. Nevertheless, the observed linear (and sometimes sub-linear) scaling of the number of significant ground and excited state PNOs are promising features that pave the way for an efficient and accurate calculation of excitation energies with higher-order coupled cluster response methods.

E. Local and non-local excitations

Of utmost importance for a reliable excited state method which exploits the locality of electron correlation is to perform equally well for excited states with different characters. In particular, excited states that have a non-local character like charge transfer (CT) or Rydberg states should be ideally treated as accurately as local valence excitations (LE). For the former, less local PNOs are expected since the PNO basis should automatically adapt to the physical character of the excitation. To test the self-adaptive behavior of PNOs we compared the first and third excited state in DBQ which are CT and LE states, respectively. Recent investigations of DBQ by Goerigk and Grimme[62] revealed that the $S_0 \rightarrow S_1$ transition exhibits a significant CT character and its excitation energy calculated with CIS(D)/def2-TZVPP deviates from the experimental value, though determined in solution, by only 0.05 eV. In Fig. 8, we plotted the most dominant occupied and virtual NTOs of S_1 and S_3. For S_1 the occupied NTO mainly occupies the two adjacent phenylene rings twisted by 29°, whereas the virtual NTO is just localized at one of them. In contrast to this, the most dominant occupied and virtual NTO of S_3 are mainly located at the same phenylene ring. Thus, the analysis

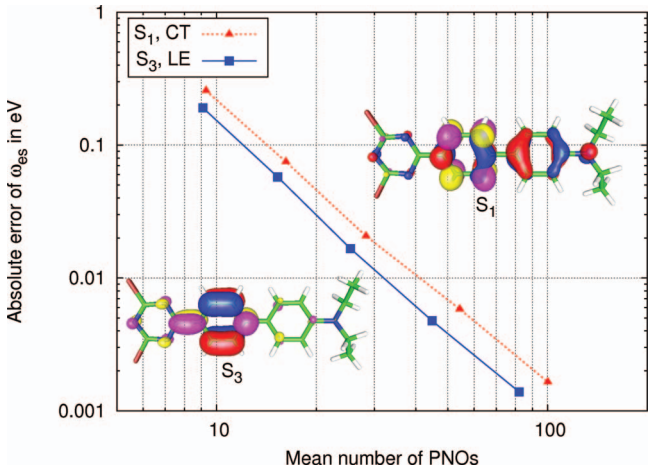


FIG. 8. Absolute PNO errors of the ω_{es} contribution to vertical CIS(D)/def2-TZVPP excitation energies in eV of the first S_1 and third excited state S_3 of DBQ (43 atoms) as a function of the mean number of PNOs. The occupied orbitals are localized by PM. The five data points in each graph correspond to PNO thresholds T_{PNO} of 1×10^{-n} with $n = 6, \ldots, 10$ as the number of PNOs increases. The most dominant occupied (red and blue) and virtual NTO (yellow and magenta) are plotted for the charge transfer (CT) S_1 and locally excited state (LE) S_3.

Downloaded 09 Jan 2012 to 134.147.252.238. Redistribution subject to AIP license or copyright; see http://jcp.aip.org/about/rights_and_permissions

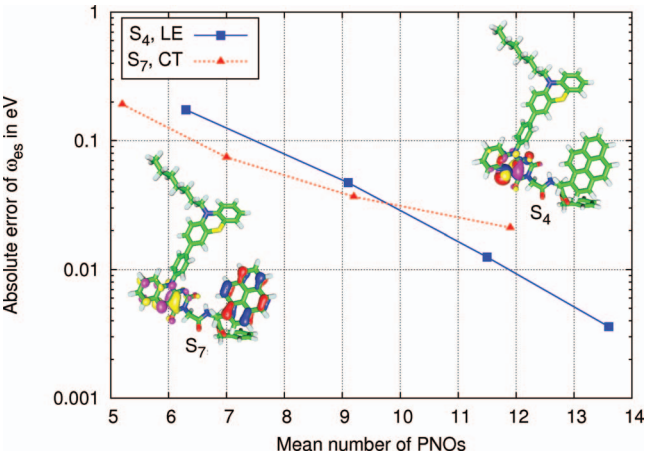


FIG. 9. Absolute PNO errors of the ω_{es} contribution to vertical CIS(D)/cc-pVDZ excitation energies in eV of the fourth S_4 and seventh excited state S_7 of triad (127 atoms) as a function of the mean number of PNOs. The occupied orbitals are localized by PM. The four data points in each graph correspond to PNO thresholds T_{PNO} of 1×10^{-n} with $n = 6, \ldots, 9$ as the number of PNOs increases. The most dominant occupied (red and blue) and virtual NTO (yellow and magenta) are plotted for the charge transfer (CT) S_7 and locally excited state (LE) S_4.

of the dominant NTOs underlines the CT character of the $S_0 \rightarrow S_1$ and the LE character of the $S_0 \rightarrow S_3$ transition (both $\pi \rightarrow \pi^*$). The truncation error of ω_{es} as a function of the mean number of excited state PNOs per pair is also shown in Fig. 8 for both excited states, where the occupied orbitals were localized with the PM procedure. Despite the clear non-local character of S_1 the number of excited state PNOs is for this state just insignificantly larger than for S_3. Due to compensating errors of the ground (ω_{gs}) and excited state (ω_{es}) contributions to the excitation energy the CT state has for a PNO threshold of 10^{-8} even a slightly smaller absolute error (0.003 eV) than the LE state (0.005 eV).

As another test case we have investigated the fourth (LE) and seventh (CT) excited state of a phenothiazine-isoalloxazine-pyrene triad taken from Ref. 27, which for convenience will be referred to as triad. The most dominant occupied and virtual NTOs are plotted in Fig. 9 for S_4 and S_7. In case of S_4, the excitation is restricted to the isoalloxazine chromophore ($n \rightarrow \pi^*$). Compared to the S_1 state of DBQ where the transition occurs between neighbored phenylene groups, for S_7 the electron is excited from the pyrene unit to the distant isoalloxazine chromophore ($\pi \rightarrow \pi^*$). Therefore, the charge transfer character of this state is much more pronounced than for S_1 in DBQ. Charge transfer transitions between distant chromophores are often accompanied by a large correlation contributions to the excitation energy which is also observed for S_7 of the triad. For this state the contribution from the excited state doubles amplitudes to the excitation energy (ω_{es}) amounts at the CIS(D) level to −7.01 eV which is much larger than ω_{es} of S_4 (−4.37 eV). This also affects the convergence of the PNO expansion of the excited state doubles amplitudes. Up to an error of 0.04 eV in ω_{es} the mean number of PNOs for S_7 is even smaller than for S_4 as can be seen from Fig. 9. Beyond this point, as one might expect the ω_{es} contribution converges slowly with the number of PNOs. Nevertheless, with on average only 12 PNOs per pair and only 0.2 % of the excited state doubles amplitudes expanded in PNOs (5 times smaller than for the ground state) ω_{es} is converged within 0.02 eV (and the total error in $\omega^{(2)}$ within 0.016 eV).

Of course, the slow convergence of ω_{es} with the number of PNOs is an unpleasant, though physically understandable, feature of such extreme charge transfer states. However, one should note that an improved accuracy can be obtained either by choosing different PNO thresholds for ground and excited state PNOs or by truncating PNOs according to an energy rather than an occupation number based criterion. This will be investigated in forthcoming work.

F. Comparison with domain based local methods

Domain based local CC2 methods have recently become an efficient tool for the computation of excitation energies for a variety of excited states exhibiting a local and non-local character.[28] A reasonable accuracy has been achieved where differences between local and canonical CC2 excitation energies are not larger than 0.1 eV. Encouraged by this, we have compared in Table II the ratio of the number of doubles amplitudes in the truncated PNO and the full virtual space r_D as well as the error in excitation energies $\Delta\omega$ of the LPNO-CIS(D) method with the results from local CC2 from Ref. 27. In analogy to Secs. IV A and IV B, we have selected for the cc-pVDZ and cc-pVTZ basis set a subset of states where the CIS(D) and CC2 vertical excitation energies differ by less than 1 eV and are dominated by the same orbital transitions in the CIS and CC2 excited state singles amplitudes. As can be seen from Table II the ratio of the doubles amplitude dimensions for LPNO-CIS(D) exceeds the one of local CC2 only for one state, namely S_2 in N-acetyl-glycine calculated with the cc-pVDZ basis set, and only for a rather small PNO threshold ($T_{PNO} = 1 \times 10^{-10}$). With this threshold, we obtained for all the states in the test set absolute errors less than 0.0005 eV in the excitation energy which is without doubt far more accurate than the intrinsic accuracy of the methods. As has been noted before, a good balance between accuracy and efficiency is achieved by a PNO threshold of $T_{PNO} = 1 \times 10^{-8}$ which results in ratios of the doubles amplitude dimension as well as errors in the excitation energies which compared to local CC2 are both one order of magnitude smaller.

It should, however, be noted that a comparison between local CC2 and LPNO-CIS(D) has to be made with caution. First of all, we intend to use state-specific PNOs introduced in Sec. II as an approximation within the framework of higher-order coupled cluster response methods. In principle, this requires an error analysis for these methods, which are not yet available. For such methods, the calculation of excitation energies with CIS(D)-PNOs requires the assignment of CIS to, e.g., CCSD states or an adaption of the PNO space during the solution of the eigenvalue problem for excited states. Another issue might be the comparison of efficiency. On the one hand, we could show that the virtual space is much more compact when constructed from PNOs rather than PAOs. On the other hand, the PNO construction is a $\mathcal{O}(N^5)$ step which becomes a

Downloaded 09 Jan 2012 to 134.147.252.238. Redistribution subject to AIP license or copyright; see http://jcp.aip.org/about/rights_and_permissions

TABLE II. Truncation errors of excitation energies $\Delta\omega$ in eV and relative dimension of the doubles amplitudes r_D of local CC2 (taken from Ref. 27) and LPNO-CIS(D) compared with their canonical counterpart using the cc-pVDZ and cc-pVTZ basis set. For LPNO-CIS(D) the occupied orbitals were localized with the PM localization and the PNO threshold T_{PNO} was set to 10^{-n} with $n = 6, 8,$ and 10.

		cc-pVDZ								cc-pVTZ							
				LPNO-CIS(D)								LPNO-CIS(D)					
		LCC2			$n_{\bar{a}}^{ij} > 10^{-6}$		$n_{\bar{a}}^{ij} > 10^{-8}$		$n_{\bar{a}}^{ij} > 10^{-10}$		LCC2			$n_{\bar{a}}^{ij} > 10^{-6}$		$n_{\bar{a}}^{ij} > 10^{-8}$		$n_{\bar{a}}^{ij} > 10^{-10}$	
Molecule	S_{CC2}	r_D	$\Delta\omega$	S_{CIS}	r_D	$\Delta\omega$	r_D	$\Delta\omega$	r_D	$\Delta\omega$	r_D	$\Delta\omega$	S_{CIS}	r_D	$\Delta\omega$	r_D	$\Delta\omega$	r_D	$\Delta\omega$
N-acetyl-glycine	1	29	−0.013	1	0.5	0.0026	4.3	−0.0003	20	0.0001	28	0.006	1	0.2	0.0117	1.8	−0.0008	11	<0.0001
	2	27	0.013	2	0.4	0.0001	3.3	0.0002	31	0.0003	15	0.032	2	0.1	0.0081	1.4	−0.0001	8.4	0.0001
	3	65	0.005	3	0.8	0.0160	7.5	0.0002	31	<0.0001	46	0.076	/	...	...	...	...	...	...
Propan-amide	1	54	0.001	1	1.9	−0.0008	13	−0.0004	48	<0.0001	31	0.025	1	0.6	0.0043	5.6	−0.0007	27	<0.0001
"Dipep-tide"	1	22	−0.019	1	0.3	0.0034	2.4	−0.0002	12	<0.0001	19	0.011	1	0.1	0.0132	1.0	−0.0006	6.5	>−0.0001
	2	23	−0.000	2	0.3	0.0049	2.7	−0.0001	14	<0.0001	19	0.000	2	0.1	0.0130	1.0	−0.0001	7.0	−0.0001
"β-dipep-tide"	1	15	−0.030	1	0.2	−0.0048	2.2	−0.0014	11	0.0004	12	0.013	1	0.1	−0.0020	0.8	−0.0022	5.6	0.0003
	2	9	−0.012	2	0.1	0.0033	1.5	−0.0002	7.8	0.0001	11	0.003	2	<0.1	0.0131	0.6	−0.0004	4.0	<0.0001
"Tripep-tide"	1	7	−0.019	1	0.1	0.0033	0.6	−0.0002	3.2	0.0001	6	0.011	1	<0.1	0.0132	0.3	−0.0006	1.7	<0.0001
trans-urocanic acid	1	43	0.010	2	0.4	0.0195	4.1	0.0008	20	0.0003	33	0.023	2	0.1	0.0399	1.6	0.0015	11	0.0002
	2	68	−0.024	1	0.8	0.0123	6.2	0.0012	23	0.0001	52	0.004	1	0.2	0.0272	2.5	−0.0003	14	<0.0001
	5	61	−0.061	...	...	...	...	...	...	...	44	0.045	4	0.1	−0.0025	1.1	0.0004	6.8	0.0001
Guanine	1	66	0.002	1	0.8	0.0182	7.2	0.0003	28	0.0001	50	0.027	1	0.2	0.0307	2.9	−0.0009	16	>−0.0001
	2	54	−0.022	2	0.4	0.0267	4.7	−0.0002	24	<0.0001	39	0.008	3	0.1	0.0448	1.8	−0.0002	13	−0.0002
	3	68	−0.002	3	0.7	0.0206	6.8	0.0011	27	0.0002	51	0.021	2	0.2	0.0331	2.6	−0.0007	15	>−0.0001
1-phenyl-pyrrole	1	36	0.012	1	0.5	0.0175	5.0	0.0005	23	−0.0001	31	0.025	1	0.1	0.0252	1.9	0.0004	12	−0.0001
DMABN	1	31	0.038	2	0.5	0.0073	4.5	0.0011	20	0.0003	27	0.057	2	0.1	0.0097	1.7	−0.0006	11	0.0001
	2	57	−0.064	1	0.6	0.0128	5.7	−0.0008	24	−0.0002	46	0.028	/	...	...	...	...	...	...
p-cresol	1	43	0.011	1	1.3	0.0067	9.6	−0.0001	32	<0.0001	37	0.025	1	0.4	0.0099	4.0	−0.0014	20	<0.0001
HPA	1	22	0.013	1	0.3	0.0128	2.7	<0.0001	14	<0.0001	18	0.030	1	<0.1	0.172	1.0	−0.0010	6.8	−0.0001
	2	10	0.011	3	0.1	0.0026	1.1	>−0.0001	6.9	0.0003	7	0.024	3	<0.1	0.0111	0.4	−0.0003	3.1	0.0001
	3	28	−0.024	2	0.3	0.0205	3.0	−0.0002	15	−0.0001	19	0.011	/	...	...	...	...	...	...
Tyrosine	1	19	0.022	1	0.2	0.0154	2.1	0.0001	12	>−0.0001	15	0.043	1	0.1	0.0197	0.8	−0.0007	5.6	−0.0001
	2	24	−0.001	3	0.1	0.0123	1.4	−0.0001	9.5	<0.0001	16	0.022	3	<0.1	0.0231	0.5	−0.0005	4.0	−0.0001
	3	33	−0.003	2	0.3	0.0271	2.5	<0.0001	14	−0.0001	23	0.013	2	0.1	0.0386	0.9	−0.0002	6.5	−0.0002
Phenyl-alanine	1	18	0.029	1	0.3	0.0248	2.3	0.0013	12	<0.0001	16	0.045	1	0.1	0.0325	0.8	0.0012	5.9	<0.0001
	2	27	0.002	3	0.1	0.0111	1.9	−0.0002	12	<0.0001	18	0.017	3	<0.1	0.0235	0.6	−0.0007	5.3	−0.0001
	3	33	−0.005	2	0.3	0.0311	2.8	0.0005	15	−0.0001	22	0.020	2	0.1	0.0408	1.0	0.0008	7.1	−0.0001
DA1	1	13	−0.024	1	<0.1	0.0663	0.2	0.0030	1.4	0.0001	...	...	...	...	...	...	...	...	...
DA2	1	3.5	−0.034	1	<0.1	0.0570	0.1	0.0029	0.4	>−0.0001	...	...	...	...	...	...	...	...	...

bottleneck for extended systems if no further approximations are made.

Nevertheless, the automatic adaption of the exited state PNO space to the physical character of the electronic excitation is a major advantage of this approach. Previous work on local CC2 and CCSD excitation energies (see Ref. 26 and 27) has shown that particularly CT states can suffer from non-negligible errors from the local correlation treatment. Improved numerical results were accomplished by using the Laplace transformation of the orbital denominators in the context of local CC2 methods,[28] where the eigenvalue problem is solved effectively by using only the untruncated singles vector. However, this procedure is limited to second-order methods like CC2 and cannot be transferred to higher-order methods like CCSD to which we are aiming.

V. CONCLUSION

In this paper, we have shown that state-specific PNOs are an attractive choice for an accurate and efficient computation of excitation energies with a truncated double excitation space. As for ground states, the number of significant PNOs scales linearly in the asymptotic limit if the

Downloaded 09 Jan 2012 to 134.147.252.238. Redistribution subject to AIP license or copyright; see http://jcp.aip.org/about/rights_and_permissions

chromophore region is extended over the whole molecule. Even a sub-linear scaling is observed if the non-chromophore part is extended but the chromophore part remains spatially confined. Unlike ground state PNOs, state-specific PNOs become most compact when the occupied orbitals are localized by Pipek-Mezey localization. Mixed orbital spaces as they have been proposed by Mata and Stoll lead to enlarged PNO spaces and are surprisingly not superior to conventional localization schemes, at least for excited state PNOs. With a PNO truncation threshold of 10^{-8} we found an accuracy of at least $\approx$0.01 eV for a large variety of locally excited states and even charge transfer states. As for the ground state, the errors seem to increase slightly with the basis set size. A pleasant feature of the excited state PNOs is that they automatically adapt to the physical character of the excited state. For pronounced charge transfer states where the excitation occurs between different chromophores we observe a reduced convergence with T_{PNO}, although the number of significant PNOs is still smaller than for the ground state. The accuracy of these states is still acceptable, though. One possibility to improve the accuracy might be an alternative truncation criterion where PNOs are selected by means of contributions to the pair correlation energy. This will be investigated in future work. In addition, we have shown that the PNO truncation errors in the excitation energy as well as the relative dimension of the truncated doubles amplitude vectors are about one order of magnitude smaller than for the local CC2 method reported in Ref. 27. Altogether, we find that state-specific PNOs are a promising approach for the development of coupled cluster response methods capable of calculating excitation energies of extended molecular systems accurately and efficiently.

ACKNOWLEDGMENTS

The authors gratefully thank Dr. Tatiana Korona and Dr. Daniel Kats for supplying the molecular structures used in Sec. IV. B.H. thanks the TURBOMOLE GmbH for financial support.

[1] H. J. Monkhorst, Int. J. Quantum Chem. **12**, 421 (1977).
[2] D. Mukherjee and P. K. Mukherjee, Chem. Phys. **39**, 325 (1979).
[3] E. Dalgaard and H. J. Monkhorst, Phys. Rev. A **28**, 1217 (1983).
[4] H. Sekino and R. J. Bartlett, Int. J. Quantum Chem., 255 (1984).
[5] H. Koch and P. Jørgensen, J. Chem. Phys. **93**, 3333 (1990).
[6] H. Koch, O. Christiansen, P. Jørgensen, and J. Olsen, Chem. Phys. Lett., **244**, 75 (1995).
[7] I. Tamm, J. Phys. USSR **9**, 449 (1945).
[8] S. M. Dancoff, Phys. Rev. **78**, 382 (1950).
[9] O. Christiansen, H. Koch, and P. Jørgensen, Chem. Phys. Lett. **243**, 409 (1995).
[10] H. Koch, H. J. A. Jensen, P. Jørgensen, and T. Helgaker, J. Chem. Phys. **93**, 3345 (1990).
[11] O. Christiansen, H. Koch, and P. Jørgensen, J. Chem. Phys. **103**, 7429 (1995).
[12] K. Hald, P. Jørgensen, J. Olsen, and M. Jaszuński, J. Chem. Phys. **115**, 671 (2001).
[13] M. Kállay and J. Gauss, J. Chem. Phys. **121**, 9257 (2004).
[14] M. Häser, Theor. Chem. Acc. **87**, 147 (1993).
[15] P. Y. Ayala and G. E. Scuseria, J. Chem. Phys. **110**, 3660 (1999).
[16] D. S. Lambrecht, B. Doser, and C. Ochsenfeld, J. Chem. Phys. **123**, 184102 (2005).
[17] B. Doser, D. S. Lambrecht, and C. Ochsenfeld, Phys. Chem. Chem. Phys. **10**, 3335 (2008).
[18] H. Stoll, Chem. Phys. Lett. **191**, 548 (1992).
[19] J. Friedrich, M. Hanrath, and M. Dolg, J. Phys. Chem. **126**, 154110 (2007).
[20] M. Ziółkowski, B. Jansík, T. Kjærgaard, and P. Jørgensen, J. Chem. Phys. **133**, 014107 (2010).
[21] P. Pulay, Chem. Phys. Lett. **100**, 151 (1983).
[22] C. Hampel and H.-J. Werner, J. Chem. Phys. **104**, 6286 (1996).
[23] M. Schütz and H.-J. Werner, Chem. Phys. Lett. **318**, 370 (2000).
[24] M. Schütz and H.-J. Werner, J. Chem. Phys. **114**, 661 (2001).
[25] T. D. Crawford and R. A. King, Chem. Phys. Lett. **366**, 611 (2002).
[26] T. Korona and H.-J. Werner, J. Chem. Phys. **118**, 3006 (2003).
[27] D. Kats, T. Korona, and M. Schütz, J. Chem. Phys. **125**, 104106 (2006).
[28] D. Kats and M. Schütz, J. Chem. Phys. **131**, 124117 (2009).
[29] R. A. Mata and H. Stoll, J. Chem. Phys. **134**, 034122 (2011).
[30] C. Edmiston and M. Krauss, J. Chem. Phys. **45**, 1833 (1966).
[31] W. Meyer, Int. J. Quantum Chem. **5**, 341 (1971).
[32] W. Meyer, J. Chem. Phys. **58**, 1017 (1973).
[33] P. J. Hay, J. Chem. Phys. **59**, 2468 (1973).
[34] W. Meyer, Theor. Chem. Acc. **35**, 277 (1974).
[35] R. Ahlrichs and F. Driessler, Theor. Chim. Acta **36**, 275 (1975).
[36] R. Ahlrichs, H. Lischka, V. Staemmler, and W. Kutzelnigg, J. Chem. Phys. **62**, 1225 (1975).
[37] R. Ahlrichs, F. Driessler, H. Lischka, V. Staemmler, and W. Kutzelnigg, J. Chem. Phys. **62**, 1235 (1975).
[38] R. Ahlrichs, F. Keil, H. Lischka, W. Kutzelnigg, and V. Staemmler, J. Chem. Phys. **63**, 455 (1975).
[39] W. Meyer and P. Rosmus, J. Chem. Phys. **63**, 2356 (1975).
[40] R. Ahlrichs, H. Lischka, B. Zurawski, and W. Kutzelnigg, J. Chem. Phys. **63**, 4685 (1975).
[41] W. Meyer, P. C. Hariharan, and W. Kutzelnigg, J. Chem. Phys. **73**, 1880 (1980).
[42] F. Neese, F. Wennmohs, and A. Hansen, J. Chem. Phys. **130**, 114108 (2009).
[43] F. Neese, A. Hansen, and D. G. Liakos, J. Chem. Phys. **131**, 064103 (2009).
[44] O. Vahtras, J. Almlöf, and M. Feyereisen, Chem. Phys. Lett. **213**, 514 (1993).
[45] M. Feyereisen, G. Fitzgerald, and A. Komornicki, Chem. Phys. Lett. **208**, 359 (1993).
[46] D. Tew, B. Helmich, and C. Hättig, J. Chem. Phys. **135**, 074107 (2011).
[47] M. Head-Gordon, R. J. Rico, M. Oumi, and T. J. Lee, Chem. Phys. Lett. **219**, 21 (1994).
[48] H. Koch, A. S. de Merás, T. Helgaker, and O. Christiansen, J. Chem. Phys. **104**, 4157 (1996).
[49] A. V. Luzanov, A. A. Sukhorukov, and V. É. Umanskii, Theor. Exp. Chem. **10**, 354 (1976).
[50] R. L. Martin, J. Chem. Phys. **118**, 4775 (2003).
[51] M. Häser and R. Ahlrichs, J. Comp. Chem. **10**, 104 (1989).
[52] O. Treutler and R. Ahlrichs, J. Chem. Phys. **102**, 346 (1995).
[53] C. Hättig and F. Weigend, J. Chem. Phys. **113**, 5154 (2000).
[54] TURBOMOLE V6.3 2011, a development of University of Karlsruhe and Forschungszentrum Karlsruhe GmbH, 1989–2007, TURBOMOLE GmbH, since 2007; available from http://www.turbomole.com.
[55] A. Schäfer, C. Huber, and R. Ahlrichs, J. Chem. Phys. **100**, 5829 (1994).
[56] F. Weigend, M. Häser, H. Patzelt, and R. Ahlrichs, Chem. Phys. Lett. **294**, 143 (1998).
[57] F. Weigend and R. Ahlrichs, Phys. Chem. Chem. Phys. **7**, 3297 (2005).
[58] T. H. Dunning, J. Chem. Phys. **90**, 1007 (1989).
[59] R. A. Kendall, T. H. Dunning, and R. J. Harrison, J. Chem. Phys. **96**, 6796 (1992).
[60] F. Weigend, A. Köhn, and C. Hättig, J. Chem. Phys. **116**, 3175 (2002).
[61] M. Schreiber, M. R. Silva-Junior, S. P. A. Sauer, and W. Thiel, J. Chem. Phys. **128**, 134110 (2008).
[62] L. Goerigk and S. Grimme, J. Chem. Phys. **132**, 184103 (2010).
[63] See supplementary material at http://dx.doi.org/10.1063/1.3664902 for input structures and states of our benchmark set.
[64] J. Pipek and P. G. Mezey, J. Chem. Phys. **90**, 4916 (1989).
[65] S. F. Boys, Rev. Mod. Phys. **32**, 296 (1960).
[66] J. M. Foster and S. F. Boys, Rev. Mod. Phys. **32**, 300 (1960).
[67] M. R. Silva-Junior, S. P. Sauer, M. Schreiber, and W. Thiel, Mol. Phys. **108**, 453 (2010).

Downloaded 09 Jan 2012 to 134.147.252.238. Redistribution subject to AIP license or copyright; see http://jcp.aip.org/about/rights_and_permissions